Quantum Yield for ClOO Formation following Photolysis of Aqueous OClO

Carsten L. Thomsen,‡ Philip J. Reid,† and Søren R. Keiding*,‡

Contribution from the Department of Chemistry, University of Aarhus, Langelandsgade 140, DK-8000 Århus C, Denmark, and Department of Chemistry, Box 351700, University of Washington, Seattle, Washington 98195

Received June 15, 2000. Revised Manuscript Received September 7, 2000

Abstract: The photochemistry of chlorine dioxide (OClO) in aqueous solution was investigated by femtosecond transient absorption spectroscopy. Following the photoexcitation of OClO at 400 nm, the transient absorption dynamics were probed in the spectral range from 400 to 220 nm. As expected from earlier studies, the main photolytic products ClO + O, formed with a quantum yield of ∼90%, disappear through fast geminate recombination producing OClO in the electronic ground state. The total quantum yield for chlorine atom production is (Φ_{Cl}) ∼10%, with the chlorine atom production occurring through two competing processes. The dominant channel for chlorine atom production involves the formation of a short-lived intermediate on a ∼6 ps time scale with a quantum yield of 8 ± 2%. The remaining 2 ± 1% is formed through the formation and decomposition of ClOO. The lifetime of ClOO was found to be ∼0.32 ns, in very good agreement with the result of a recent time-resolved resonance Raman study. Finally, the UV absorption spectrum for aqueous ClOO is reported and compared with previously reported spectra obtained in condensed media.

Introduction

The photochemistry of chlorine dioxide (OClO) is of current interest due to its participation in the stratospheric reactive chlorine reservoir as well as its potential role in ozone depletion.[1−6] An outline of the three distinct photochemical pathways available to OClO following photoexcitation is presented in reactions 1−3.

$$OClO(X^2B_1) \xrightarrow{h\nu} ClO(^2\Pi) + O(^3P_g) \quad (1)$$

$$OClO(X^2B_1) \xrightarrow{h\nu} Cl(^3P_u) + O_2(^3\Sigma_g^-, ^1\Delta_g) \quad (2)$$

$$OClO(X^2B_1) \xrightarrow{h\nu} ClOO \xrightarrow{\Delta} Cl(^2P_u) + O_2(^3\Sigma_g^-) \quad (3)$$

Since the environmental impact of OClO arises from its ability to produce atomic chlorine, knowing the quantum yield for reactions 2 and 3 is essential if the environmental impact of OClO in both homogeneous and heterogeneous media is to be predicted. This has served as an inspiration for numerous experimental and theoretical investigations of OClO in both gas and condensed phases.[1−37]

When OClO is photolyzed in the gas phase with near-ultraviolet light, ClO + O is the dominant product, whereas only a moderate yield of chlorine atoms is observed.[8−15] It has been suggested that photolytic formation of Cl + O_2 via isomerization to ClOO could contribute significantly to the catalytic destruction of ozone.[1] The suggested formation of ClOO is still controversial, however, and this species has not been observed experimentally in the gas phase. The photochemistry of OClO in low-temperature matrixes is completely different from that in the gas phase. Specifically, the quantum yield (Φ_{Cl}) for chlorine formation in the gas phase is ≤4%, but increases to unity in low-temperature matrixes.[9,16−19,42] Furthermore, the formation of chlorine atoms occurs through the thermal decomposition of ClOO formed by either direct photoisomerization of OClO or by geminate recombination of primary photoproducts as ClO + O or Cl + O_2 inside the matrix cage.[18−23] It should be noted that the thermodynamically more

* To whom correspondence should be addressed. E-mail: keiding@kemi.aau.dk.

‡ University of Aarhus.

† University of Washington.

(1) Vaida, V.; Solomon, S.; Richard, E. C.; Rühl, E.; Jefferson, A. *Nature* **1989**, *342*, 405−408.

(2) Vaida, V.; Simon, J. D. *Science* **1995**, *268*, 1443−1448.

(3) Rowland, F. S. *Annu. Rev. Phys. Chem.* **1991**, *42*, 731.

(4) Burkholder, J. B.; Talukdar, R. K.; Ravishankara, A. R. *Geophys. Res. Lett.* **1994**, *21*, 585.

(5) Solomon, S.; Sanders, R. W.; H. L. Miller, J. *J. Geophys. Res.* **1990**, *95*, 13807.

(6) Sessler, J.; Chipperfield, M. P.; Pyle, J. A.; Toumi, R. *Geophys. Res. Lett.* **1995**, *22*, 687.

(7) Vaida, V.; Goudjil, K.; Simon, J. D.; Flanders, B. N. *J. Mol. Liq.* **1994**, *61*, 133−152.

(8) Rühl, E.; Jefferson, A.; Vaida, V. *J. Phys. Chem.* **1990**, *94*, 4.

(9) Davis, H. F.; Lee, Y. T. *J. Chem. Phys.* **1996**, *105*, 8142−8163.

(10) Bishenden, E.; Donaldson, D. J. *J. Chem. Phys.* **1993**, *99*, 3129.

(11) Baumert, T.; Herek, J. L.; Zewail, A. H. *J. Chem. Phys.* **1993**, *99*, 4430−4440.

(12) Delmdahl, R. F.; Bakker, B. L. G.; Parker, D. H. *J. Chem. Phys.* **2000**, *112*, 5298−5300

(13) Kreher, C. J.; Carter, R. T.; Huber, J. R. *J. Chem. Phys.* **1999**, *110*, 3309−3319

(14) Delmdahl, R. F.; Ullrich, S.; Gericke, K. H. *J. Phys. Chem. A* **1998**, *102*, 7680−7685

(15) Kreher, C. J.; Carter, R. T.; Huber, J. R. *Chem. Phys. Lett.* **1998**, *286*, 389−397

(16) Lawerence, W. G.; Clemitshaw, K. C.; Apkarian, V. A. *J. Geophys. Res.* **1990**, *95*, 18591.

(17) Lanzendorf, E. J.; Kummel, A. C. *Geophys. Res. Lett.* **1996**, *23*, 1251.

(18) Pursell, C. J.; Conyers, J.; Alapat, P.; Parveen, R. *J. Phys. Chem.* **1995**, *99*, 10433−10437.

(19) Adrian, F. J.; Bohandy, J.; Kim, B. F. *J. Chem. Phys.* **1986**, *85*, 2692−2698.

(20) Rochkind, M. M.; Pimental, G. C. *J. Chem. Phys.* **1967**, *46*.

(21) Arkell, A.; Schwager, I. *J. Am. Chem. Soc.* **1967**, *89*, 5999−6006.

(22) Johansson, K.; Engdahl, A.; Nelander, B. *J. Phys. Chem.* **1993**, *97*, 9603−9606.

10.1021/ja002148o CCC: $19.00
Published on Web 12/06/2000

stable isomer ClOO is expected to be the terminal product found within an inescapable cavity at sufficiently low temperature regardless of its mechanism of formation (i.e., whether it is formed by concerted isomerization or via recombination of the primary fragments).[24] Hence, OClO is expected to be quantitatively converted into its asymmetrical isomer ClOO in solid media, which in turn readily decomposes into Cl + O_2 at ambient temperature. The quantum yield of chlorine formation in aqueous solution is intermediate between the gas-phase and matrixes values, with $\Phi_{Cl} \sim 10\%$.[31,34,39−40] Despite the well-determined Cl quantum yield, the formation mechanisms and time scale of chlorine production in solution phase remains controversial.

Studies of OClO solution-phase photochemistry have attempted to identify the specific solvent−solute interactions responsible for the phase-dependent quantum yield of the photoproducts. The solution-phase photochemistry of OClO was pioneered by Simon and co-workers using picosecond flash photolysis.[30−33] The current understanding of the photolysis of OClO in solution, however, has been obtained using femtosecond transient absorption and time-resolved resonance Raman experiments.[34−41] It is now well established that the dominant primary photoproduct channel is the ClO + O, reaction 1, occurring with a ∼ 90% yield.[34−41] These studies also show that the majority of the ClO and O photoproducts undergo geminate recombination to form vibrationally excited OClO in the electronic ground state as a result of the solvent caging effect. The subsequent vibrational relaxation of the hot OClO molecule on the ground-state potential surface occurs with a time constant of ∼10 ps.

$$ClO(^2\Pi) + O(^3P_g) \rightarrow OClO^*(X^2B_1) \rightarrow OClO(X^2B_1) \quad (4)$$

Transient absorption spectroscopy covering the first 50 ps of the photolysis of OClO indicates that the production of chlorine atoms occurs through a short-lived precursor within 15 ps and with a total quantum yield of $\Phi_{Cl} \sim 10\%$.[34,38] Thus, the current understanding of the production of chlorine atoms from photolysis of aqueous OClO does not involve any long-lived ClOO isomer.

Even though the isomer ClOO has been proposed to be a photoproduct of aqueous OClO for the past decade, it was not until very recently that its existence was unambiguously established. By using two-color, time-resolved resonance Raman (TRRR) spectroscopy, the formation of ClOO following photoexcitation of aqueous OClO was confirmed.[41] The integrated scattering intensity of ClOO was best modeled by a sum of two exponentials resulting in appearance and decay time constants of 28 ± 5 ps and 0.40 ± 0.05 ns, respectively. In addition, a delay of 13 ± 2 ps was included to reproduce the absence of ClOO scattering at early times. These TRRR results were the first direct evidence for the formation and decomposition of ClOO in aqueous solution, and indicate that the current model for chlorine formation should be extended. The quantum yield for ClOO formation could not be determined in the TRRR experiment. Therefore, we have revisited the photolysis of aqueous OClO with the aim of studying the contribution from ClOO in the formation of atomic chlorine.

In this work, we present femtosecond transient absorption data of aqueous OClO. The photoproduct formation following photoexcitation at 400 nm is monitored over the entire spectral range from 400 to 220 nm on an absolute optical density scale, with emphasis on the dynamics occurring at long time. In contrast to earlier studies, this allows the simultaneous monitoring of the decomposition and formation of all photoproducts, including ClOO. In agreement with earlier femtosecond work on aqueous OClO, it is observed that the majority (∼90%) of the photoexcited OClO molecules dissociate into ClO and O, with geminate recombination of these products resulting in the formation of vibrationally excited OClO. In addition, it is observed that most of the chlorine atoms are produced on a ∼6 ps time scale with a quantum yield of 8 ± 2%, whereas 2 ± 1% is formed through the formation and decomposition of ClOO. The decomposition of ClOO occurs with a time constant of ∼0.32 ns in agreement with recent time-resolved resonance Raman studies. The femtosecond data presented here represent the first direct measurement of the quantum yield for ClOO formation in aqueous solution, and significantly clarify the role of this controversial species in the mechanism for chlorine formation in aqueous solution.

Experimental Section

The details of the ultrafast transient absorption spectrometer have been presented elsewhere.[38,43] Briefly, a regenerative amplified Titanium:Sapphire laser producing 90-fs, 750-μJ pulses centered at 800 nm with a repetition rate of 1 kHz was employed in this work. The fundamental beam at 800 nm was frequency doubled in a 0.5-mm-thick BBO crystal to generate the 400-nm pump pulse used for the photolysis of OClO. The pump pulse was sent through a variable delay line and a wave-plate rotated the polarization of the pump pulse 54.7° relative to that of the probe pulse before it was weakly focused into a sample flow cell. The pump pulse energy was typically 50 μJ with a spot diameter of 1.3 mm at the sample and it was modulated at 0.5 kHz, phase-locked to the 1 kHz repetition rate of the regenerative amplifier. The results obtained were independent of the pump pulse energy indicating negligible multiphoton absorption.[38−40] The probe pulse was generated using a combination of second harmonic generation and sum-frequency mixing of a supercontinuum generated by focusing

(23) Müller, H. S. P.; Willner, H. *J. Phys. Chem.* **1993**, *97*, 10589−10598.
(24) Brusa, M. A.; Perissinotti, L. J.; Churio, M. S.; Colussi, A. J. *J. Photochem. Photobiol. A* **1996**, *101*, 105−111.
(25) Mauldin, R. L., III; Burkholder, J. B.; Ravishankara, A. R. *J. Phys. Chem.* **1992**, *96*, 2582−2588.
(26) Gole, J. L. *J. Phys. Chem.* **1980**, *84*, 1333−1340.
(27) Jafi, J. A.; B. H. Bauschlicher, J.; Phillips, D. H. *J. Chem. Phys.* **1985**, *83*, 1693−1701.
(28) Peterson, K. A.; Werner, H.-J. *J. Chem. Phys.* **1992**, *96*, 8948−8961.
(29) Peterson, K. A.; Werner, H.-J. *J. Chem. Phys.* **1996**, *105*, 9823−9832.
(30) Dunn, R. C.; Richard, E. C.; Vaida, V.; Simon, J. D. *J. Phys. Chem.* **1991**, *95*, 6060−6063.
(31) Dunn, R. C.; Simon, J. D. *J. Am. Chem. Soc.* **1992**, *114*, 4856−4860.
(32) Dunn, R. C.; Anderson, E. J. L.; Foote, C. S.; Simon, J. D. *J. Am. Chem. Soc.* **1993**, *115*, 5307.
(33) Dunn, R. C.; Flanders, B. N.; Simon, J. D. *J. Phys. Chem.* **1995**, *99*, 7360−7370.
(34) Philpott, M. J.; Charalambous, S.; Reid, P. J. *Chem. Phys. Lett.* **1997**, *281*, 1−9.
(35) Philpott, M. J.; Hayes, S. C.; Reid, P. J. *Chem. Phys.* **1998**, *236*, 207−224.
(36) Hayes, S. C.; Philpott, M. J.; Reid, P. J. *J. Chem. Phys.* **1998**, *109*, 2596−2599.
(37) Hayes, S. C.; Philpott, M. J.; Mayer, S. G.; Reid, P. J. *J. Phys. Chem.* **1999**, *103*, 5534−5546.
(38) Thøgersen, J.; Jepsen, P. U.; Thomsen, C. L.; Poulsen, J. A.; Byberg, J. R.; Keiding, S. R. *J. Phys. Chem. A* **1997**, *101*, 3317−3323.
(39) Poulsen, J. A.; Thomsen, C. L.; Keiding, S. R.; Thøgersen, J. *J. Chem. Phys.* **1998**, *108*, 8461−8471.
(40) Thøgersen, J.; Thomsen, C. L.; Poulsen, J. A.; Keiding, S. R. *J. Phys. Chem. A* **1998**, *102*, 4186−4191.
(41) Thomsen, C. L.; Philpott, M. P.; Hayes, S. C.; Ried, P. J. *J. Chem. Phys.* **2000**.
(42) Bishenden, E.; Donaldson, D. J. *J. Phys. Chem.* **1994**, *101*, 1.
(43) Thomsen, C. L.; Madsen, D.; Keiding, S. R.; Thøgersen, J. *J. Chem. Phys.* **1999**, *110*, 3453−3462.

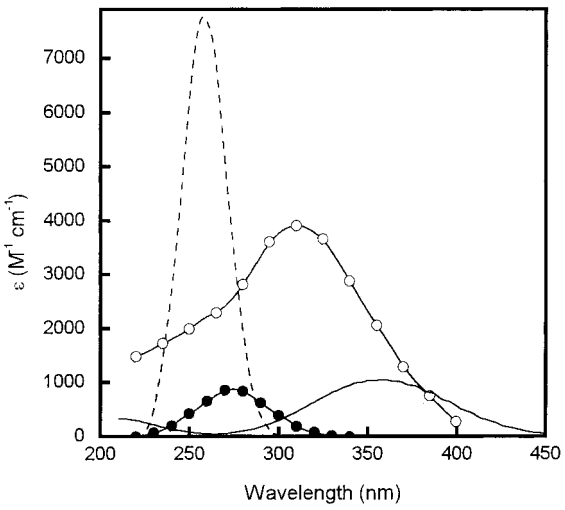

Figure 1. Absorption spectra of OClO(aq) (—), ClOO(s) (- - -), ClO(aq) (●), and the Cl:H_2O charge-transfer complex (○). The absorption spectrum of OClO(aq) was measured by us and the absolute absorption scale was taken from ref 44. The absorption spectrum of aqueous ClOO has not previously been measured, and depicted here is the ClOO spectrum measured in amorphous ice[18] calibrated with the gas-phase value for the extinction coefficient.[25] The absorption spectra of aqueous ClO and Cl:H_2O are taken from refs 45 and 46.

the residual 800 nm beam into a 2 mm ethylene glycol jet. The spectral range from 400 to 295 nm was covered by frequency doubling the white light continuum in a 1-mm -thick BBO crystal. To generate the probe wavelengths from 220 to 317 nm, the white light continuum was sum-frequency mixed with part of the 400-nm beam in a 0.2-mm-thick BBO crystal. The probe beam was separated into signal and reference beams using a beam splitter. The reference portion of the probe was sent to a detector while the remainder of the beam was sent through the sample. Both beams were spectrally filtered before they were detected by two matched photodiodes and boxcar integrators, and the ratio of the signals from the two boxcar integrators was sent to a digital lock-in amplifier referenced to the pump beam modulation. The probe wavelength was measured by a calibrated spectrometer and the instrument-response time was 300 ± 50 fs (fwhm). The pulse energy was kept well below 0.1 FJ to avoid photolysis by the probe pulse.

Aqueous solutions of OClO were prepared by mixing $NaClO_2$ and $K_2S_2O_8$ as described elsewhere.[38] The OClO solution was exchanged frequently during the series of measurements, and the flow was adjusted to ensure a fresh sample of OClO for each laser pulse. The absorbance of the OClO solution was 5 at 400 nm, the optical path length was 2 mm, and a reservoir solution of 1 L was employed. A series of measurements with different OClO concentrations showed no difference in the dynamics observed indicating no OClO clustering effects at the concentrations employed in this work.[15] Absorption spectra obtained before and after experiments were identical demonstrating that no sample degradation occurred during the course of the experiment. The overall uncertainty of the transient absorption measurements is estimated to be less than ±15% for the spectral region from 220 to 400 nm.

Results and Discussion

Static Absorption Spectra of the Species Involved. In accordance with previous work[31,40] the present results are interpreted in terms of the equilibrated spectral properties of the following potential photolytic products OClO, Cl, ClO, and ClOO (Figure 1). The near-UV ($X^2B_1 \rightarrow A^2A_2$) absorption spectrum of OClO in aqueous solution was measured on a Cary 219 spectrophotometer with 2-nm resolution. The spectrum obtained is in good agreement with previous studies where the extinction coefficient was determined to be 1050 M^{-1} cm^{-1} at 355 nm.[44] The absorption spectrum of ClOO has not been determined in aqueous solution due to the reactivity of this molecule. However, an accurate UV spectrum in the gas phase has been obtained,[25] and a spectrum extended into the visible region has been measured in solid neon.[23] These spectra agree within the limit of error.[23] The spectrum has also been measured in amorphous ice at 80 K and resembles the gas-phase and matrix-isolated spectra with only a small (≈7 nm) red shift of the absorption band.[18] This indicates the absence of large solvatochromic effects on the ClOO absorption band. Accordingly, we adopt the spectrum measured in amorphous ice calibrated with the gas-phase value for the extinction coefficient. The absorption spectra of aqueous ClO and Cl:H_2O have been well characterized spectroscopically, and the spectra depicted in Figure 1 are taken from refs 45 and 46. It should be noted that two of the potential photoproducts, O and O_2, do not have significant absorption bands over the spectral range covered in these measurements. The spectra of the three potential photoproducts Cl, ClO, and ClOO overlap to a significant extent, but since ClOO absorbs much stronger than the other products it is possible to estimate the quantum yield of each of the competitive reactions pathways 1−3 by analyzing the transient absorption spectra.

Description of Transient Absorption Data and Assignments. The photoinduced absorption, $\Delta A(\lambda,t)$ of aqueous OClO, produced by the 400-nm pump pulse was measured at 16 wavelengths in the spectral range from 220 to 400 nm. Additional transient absorption measurements were performed in the spectral range from 220 to 310 nm to better resolve the spectral behavior within the first 100 ps. Figure 2 shows the transient absorption for representative wavelengths in the region from 220 to 400 nm.

At 400 nm, a strong initial bleaching is observed which recovers to reveal a small residual depletion in optical density that persists out to the longest delays investigated. The recovery of the signal exhibits a double exponential decay with time constants of 6.0 ± 1.0 ps and 0.33 ± 0.05 ns in addition to a constant absorption signal. The time constants determined for this and other probe wavelengths are presented in Table 1. The spectral region from 400 to 320 nm covers the absorption band of the Cl:H_2O complex and the ground-state ($X^2B_1 \rightarrow A^2A_2$) electronic absorption of OClO. The strong initial bleaching observed at 400 nm is due to the removal of ground-state OClO by the pump pulse and indicates that the primary photoproducts, including the pertinent excited states of OClO, all absorb much less at 400 nm than does ground-state OClO. The nearly complete, fast recovery of the absorption at 400 nm has previously been assigned to reformation and subsequently relaxation of vibrationally excited OClO(X^2B_1) and the formation of Cl atoms.[34−41] The transient absorption signal is very sensitive to the probe wavelength and, as the wavelength is decreased, the bleaching at 400 nm is replaced by an induced absorption caused by the increasing extinction coefficient of the Cl:H_2O complex (λ_{max} = 310 nm). This is exemplified by the 320-nm transient absorption data (Figure 2). The evolution in optical density at this probe wavelength also shows a double decay with time constants of 6.3 ± 1.0 ps and 0.29 ± 0.07 ns in addition to a constant absorption signal. To investigate the spectral behavior of the induced absorption, transient absorption

(44) Stritt, F.; Friedlander, S.; Lewis, H. J.; Young, F. E. *Anal. Chem.* **1954**, *26*, 1478−1884.
(45) Kläning, U. K.; Wolff, T. *Ber. Bunsen-Ges. Phys. Chem.* **1985**, *89*, 243−245.
(46) Buxton, G. V.; Subhami, M. S. *J. Chem. Soc., Faraday Trans. 1* **1972**, *68*, 947−957.

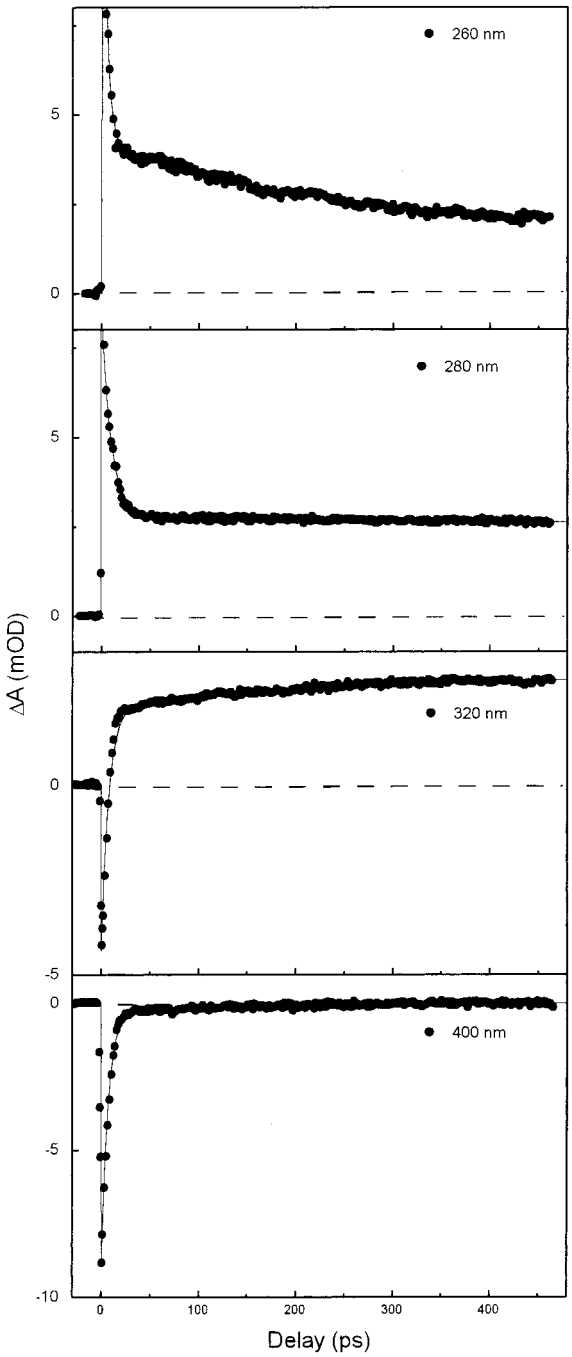

Figure 2. The transient absorption data of aqueous OClO measured in the spectral region from 400 to 220 nm following excitation at 400 nm. The probe wavelength used for each data point is labeled and the continuous curve is a fit to the measured data using a sum of two exponentials and a long-time offset convoluted with the instrument response function. The time evolution of the transient absorption data at 400 nm is dominated by the dissociation and reformation of OClO, the data at 320 nm are dominated by the production of Cl atoms, and the data at 260 nm are dominated by the decay of the ClOO isomer, Figure 1.

spectra were constructed from the individual transient absorption data, Figure 3. At short delays (3.5 ps) the spectral region between 400 and 320 nm is, as already discussed, dominated by the induced transient bleaching of the sample, whereas the transient absorption originating from the Cl:H_2O complex is seen to dominate at longer delays. The time evolution of the Cl production can be observed by investigating the transient data in the spectral range 340 to 300 nm where the absorption is dominated by the Cl:H_2O complex as exemplified in Figure 2 by the measurement at 320 nm. The spectral evolution of the transient absorption data in Figures 2 and 3 shows that the majority of the induced absorption originating from the Cl:H_2O complex appears within the first 20 ps, whereas only a very small and slow increase in the signal is observed for longer delays (>20 ps). This observation immediately suggests that Cl atoms are formed through two competing processes, reactions 2 and 3, with the majority of Cl formed within 20 ps. The time scale for the slow increase in the induced absorption in the entire spectral region from 400 to 320 nm is about ~0.32 ns (Table 1). Time-resolved resonance Raman studies have shown that this same time scale corresponds to the lifetime of aqueous ClOO.[41] This immediately suggests that a small number of Cl atoms are produced through the formation and decomposition of ClOO on a ~0.32 ns time scale.

Table 1. Kinetic Parameters Determined from the Analysis of the Transient Absorption Data of OClO in Aqueous Solution Using the Function $f(t) = A_1 \exp(-t/\tau_1) + A_2 \exp(-t/\tau_2) + A_3$ Convoluted with the Instrument-Response Time

probe (nm)[a]	A_1[b]	τ_1 (ps)	A_2	τ_2 (ns)	A_3
220	0.92 ± 0.06	2.0 ± 0.5	0.04 ± 0.02	0.08 ± 0.05	0.04 ± 0.03
230	0.89 ± 0.06	2.5 ± 0.6	0.06 ± 0.02	0.09 ± 0.06	0.05 ± 0.03
240	0.88 ± 0.07	2.5 ± 0.5	0.06 ± 0.02	0.15 ± 0.06	0.06 ± 0.02
250	0.84 ± 0.05	3.5 ± 0.5	0.08 ± 0.03	0.19 ± 0.05	0.08 ± 0.02
260	0.77 ± 0.07	4.0± 0.5	0.13 ± 0.03	0.27 ± 0.05	0.10 ± 0.03
270	0.74 ± 0.08	5.0± 1.0	0.09 ± 0.03	0.30± 0.05	0.17 ± 0.03
280	0.70 ± 0.08	9.5 ± 1.8			0.30 ± 0.05
320	−0.63 ± 0.06	6.3 ± 1.0	−0.09 ± 0.05	0.29 ± 0.05	0.28 ± 0.06
340	−0.80 ± 0.04	10.8 ± 1.2	−0.07 ± 0.04	0.31 ± 0.05	0.13 ± 0.04
360	−0.93 ± 0.02	11.9 ± 0.2	−0.02 ± 0.03	0.32 ± 0.05	0.05 ± 0.02
380	−0.98 ± 0.02	10.2 ± 0.8	−0.02 ± 0.02	0.35 ± 0.06	0.00 ± 0.02
400	−0.96 ± 0.02	6.0 ± 1.0	−0.03 ± 0.02	0.33 ± 0.05	−0.01 ± 0.02

[a] Wavelength at which the transient change in optical density was analyzed. The transient change was also measured between 290 and 310 nm, but not analyzed for multiexponential behavior. [b] Amplitudes are normalized such that $\sum |A_i| = 1$. Errors represent one standard deviation from the mean of the number of measurements performed at a given wavelength.

Interpretation of the transient absorption curves recorded at shorter wavelengths (λ_{max} < 320 nm) is rather involved since the absorption cross sections for all photoproducts (ClOO, ClO, and the Cl:H_2O complex) are substantial. Furthermore, each curve in this spectral region displays an initial sharp peak, which is due to two-photon absorption by water (one pump and one probe photon).[43] If thermal dissociation ClOO is responsible for the slow production of Cl atoms, a decrease in the absorption from 270 to 240 nm due to the decay of ClOO concentration should be observed. This is indeed the behavior observed in Figures 2 and 3. At 260 nm, an instrument-limited increase in the absorption is followed by a double exponential decay with time constants of 4.0 ± 0.5 ps and 0.27 ± 0.05 ns to a constant absorption level (Figure 2). Furthermore, the transient absorption spectra depicted in Figure 3 *unambiguously* demonstrate the formation and decay of ClOO. The transient spectrum at 50 ps has a clear absorption maximum centered around 260 nm, which can be identified as ClOO through comparison with the spectra presented in Figure 1. In the 0.46-ns spectrum, the 260-nm band has disappeared, and the absorption between 300 and 400 nm has increased consistent with Cl:H_2O complex formation. The spectra presented in Figure 3 also indicate that decomposition of ClOO occurs within 0.5 ns resulting in the production of Cl and O_2. We therefore conclude that most of the Cl atoms are formed within 20 ps, whereas a small number of Cl atoms are produced through the formation and decomposition of ClOO on a 0.32 ns time scale.

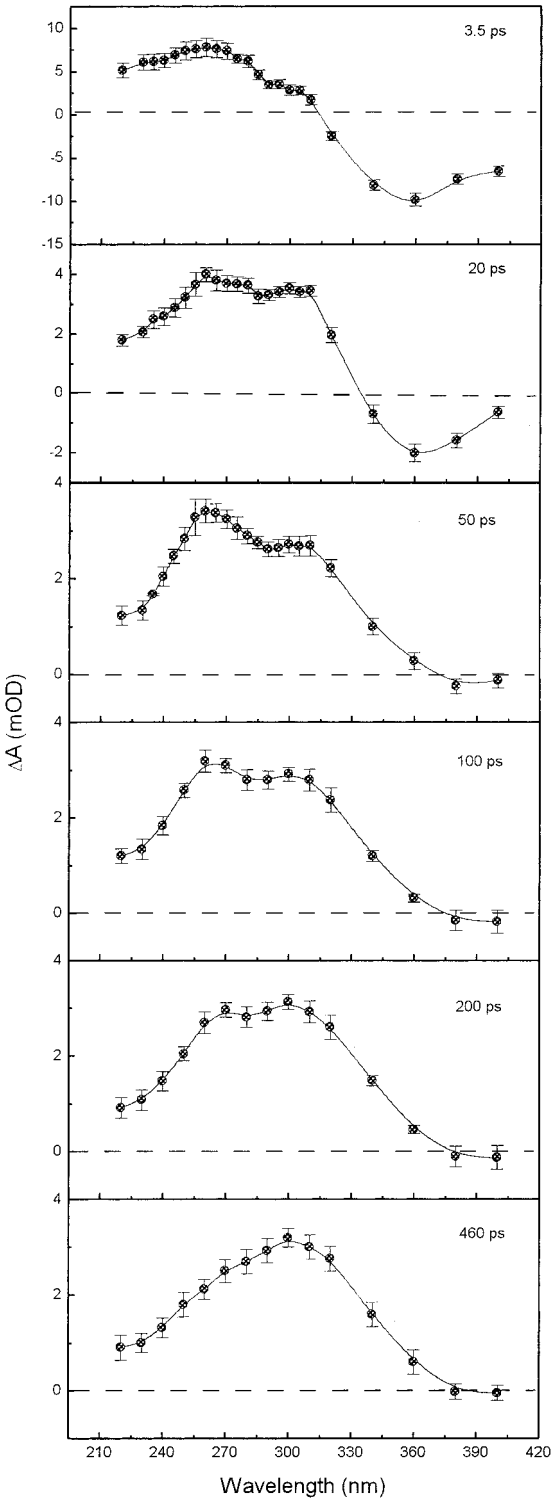

Figure 3. The transient absorption spectra of aqueous OClO measured in the spectral region from 400 to 220 nm following excitation at 400 nm. The time delay used for each spectrum is labeled. The transient spectrum at 50 ps has a clear absorption maximum centered at 260 nm, which can be identified as ClOO. In the 0.46-ns spectrum, the 260-nm band has disappeared, and the absorption between 300 and 400 nm has slightly increased consistent with $Cl:H_2O$ complex formation. By investigating the time evolution of the transient spectra in the region from 400 to 300 nm it is observed that the majority of the induced absorption originating from the $Cl:H_2O$ complex appears within the first 20 ps, indicating that the main portion of Cl atoms is not formed through the ground-state ClOO isomer.

The time-dependent signals at 270 and 250 nm show the same behavior as the 260-nm signal, but with decay constants of 0.30 ± 0.05 and 0.19 ± 0.05 ns, respectively. As the probe pulse is tuned to shorter wavelengths, the time-dependent signals decay faster and the long-time absorption signal decreases (Table 1). From the equilibrium spectra, depicted in Figure 1, it is seen that ClOO has maximum absorption around 260 nm with a small absorption between 240 and 220 nm. The slow part of these transients decays at a decreasing rate when going from 220 to 240 nm, and approaches that of the 260-nm transient. This spectral narrowing of the ClOO transient with time is thus similar to what is expected for a vibrationally relaxing species and suggests that ClOO is formed in a vibrationally excited state. The decay in the transient absorption signal in the spectral region around the ClOO absorption band might contain contributions from both vibrational relaxation and thermal decomposition of ClOO.

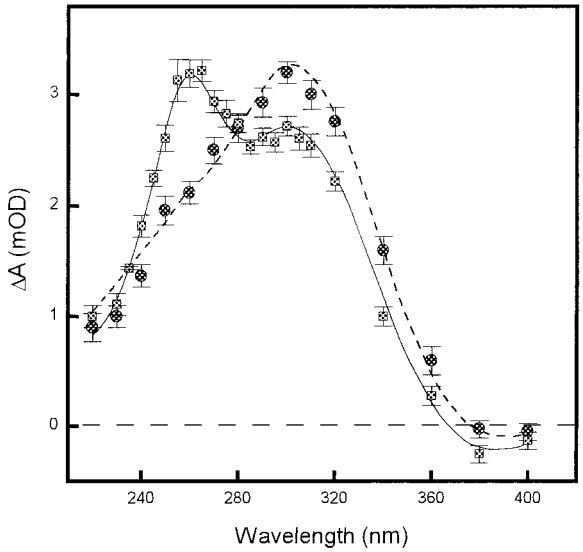

Figure 4. Transient absorption spectra measured 50 ps (■) and 0.46 ns (●) after excitation. The quantum yield for each of the reactions channels is obtained using the spectra depicted in Figure 1 and an initial concentration obtained from the 400 nm data (see details in the text). The spectrum at 50 ps is overlade (—) with the spectrum obtained using a quantum yield for direct Cl and ClOO formation of 8 ± 2% and 2 ± 1%, respectively, where a 3 ± 2% quantum yield for ClO was assumed. The remaining 87 ± 5% ClO + O was assumed to geminately recombine on a subpicosecond time scale to reform OClO. The spectrum at 0.46 ns is overlade (- - -) with the spectrum obtained using the same condition as describe above, but also including the result that ClOO decomposes to form Cl on a ∼0.32 ns time scale.

The transient absorption data at 280 nm shown in Figure 2 demonstrate that the long-time absorption signal is constant after 50 ps, indicating an isosbestic point where the absorptions originating from ClOO and the $Cl:H_2O$ complex are comparable, in agreement with the spectra shown in Figure 1. The isosbestic point at this wavelength indicates that the solution-phase spectrum of ClOO is very similar to the amorphous ice spectrum depicted in Figure 1.

Quantum Yield for ClOO Formation. To further justify the assignments made above, the measured absorption spectra obtained at delays of 50 ps and 0.46 ns after the photolysis are presented in Figure 4. The quantum yield for each of the four reactions, eq 1−4, including the two proposed reactions leading to Cl formation, can be extracted from the measured transient data using the known photoproduct extinction coefficients (Figure 1). When analyzing the spectra, it is assumed that all the species have become fully thermalized by 50 ps, so that the extinction coefficient (ϵ_i) of the equilibrated species applies. Furthermore, it is assumed in this analysis that the initial

concentration of photoexcited OClO can be found using the initial bleaching at 400 nm. Taking the maximum bleaching at 400 nm ($\Delta A(400\text{ nm}) = -0.008$, Figure 2) to indicate the initial, photoinduced deficit of ground-state OClO, and hence the initial concentration of photoexcited OClO, we obtain $\Delta[\text{OClO}]_{t=0} \approx 5 \times 10^{-5}$ M. In the absence of significant hole-burning, the absolute value of $\Delta[\text{OClO}]_{t=0}$ is a lower limit since we have assumed that none of the photoproducts or excited states of OClO present absorb at 400 nm. The spectra are analyzed using the constraint that the total concentration of all the photoproducts equals the residual concentration of OClO that has not disappeared via fast geminate recombination of ClO and O:

$$\Delta[\text{OClO}](t) = [\text{Cl}](t) + [\text{ClO}](t) + [\text{ClOO}](t) \qquad (5)$$

Furthermore, we assume that the transient absorption spectrum $\Delta A_{\lambda,t}$ can be expressed simply as:

$$\Delta A_{\lambda,t} = d_{\text{OClO}}\{\epsilon_{\text{Cl}}[\text{Cl}] + \epsilon_{\text{ClO}}[\text{ClO}] + \epsilon_{\text{ClOO}}[\text{ClOO}] - \epsilon_{\text{OClO}}\Delta[\text{OClO}]\}_{\lambda,t} \qquad (6)$$

where d is the thickness of the sample and ϵ_i is the extinction coefficient of the equilibrated species involved. The concentration of all the photoproducts is derived from the concentration of initially excited OClO molecules and the static spectra shown in Figure 1. Finally the quantum yield defined as $\Phi(X)/[X]/\Delta[\text{OClO}]_{t=0}$ where X = Cl, ClO, and ClOO is calculated. From this analysis, we obtain the quantum yields for ClOO of 2 ± 1%, Cl of 8 ± 2%, and ClO of 3 ± 2%. The analysis also shows that the majority of photoexcited OClO (87 ± 5%) reforms within 50 ps in agreement with previous femtosecond studies.[34−41] The induced absorption signal at 0.46 ns is assumed to be due to the production of Cl and residual ClO that has not recombined, whereas all ClOO is assumed to have decayed. The contribution to the total absorption from the small amount of ClOO that has yet not decayed at this time is insignificant and has therefore, within experimental error, no influence on the final quantum yields. Hence, the spectrum at 0.46 ns can be reproduced by assuming quantum yields for Cl and ClO formation of 10 ± 3% and 3 ± 2%, respectively. The obtained quantum yields at 50 ps and 0.46 ns clearly demonstrate the relationship between the decay of ClOO and the formation of Cl at long delays. This is in agreement with estimates of the barrier for thermal dissociation of ClOO along the Cl−O coordinate of only 0.26 eV.[7,27] In our analysis, diffusive geminate recombination on a long time scale between the primary photoproducts has been neglected. Previous studies of diffusion-limited geminate recombination have shown that the primary dynamics happen within the first 30 ps, which is consistent with our model.[47,48] This assumption is further supported by the fact that the majority of the ClO and O fragments geminately recombine within the first picosecond.[34−41] It is important to recall that the spectrum used to represent ClOO was that obtained in amorphous ice calibrated with the absolute scale from recent gas-phase measurements. The ability of this spectrum to completely reproduce the short time (50 ps) optical density decay observed here implies that the solution-phase spectrum of ClOO is similar to that obtained in amorphous ice. This is further supported by the observed isosbestic point at 280 nm, indicating the absence of large solvent effects on the ClOO absorption band. It should be noted that the absolute value of the ClOO extinction coefficient might change when going from gas to solution phase. However, within the uncertainty of our data, the quantum yield for ClOO formation is equaled by the increase in the quantum yield of Cl atoms when going from 50 ps to 0.46 ns. Hence, the reported quantum yields and the shape of the ClOO spectrum in water can be obtained self-consistently from the experimental data without any prior knowledge or assumptions concerning the ClOO spectrum in ice. The ClOO spectrum obtained is instead critically dependent on the shape and extinction coefficient of the Cl:H_2O spectrum and we estimate an uncertainty on the ClOO extinction coefficient on the order of ±25%

The analysis of the transient absorption spectra presented here indicates that the current model for Cl production in aqueous solution should be extended. Thus, in this model the chlorine atoms are only produced through a short-lived intermediate with a lifetime of 6 ps.[34,38−39] However, the results presented here indicate that two channels are involved in the Cl production, with the majority of Cl formed within 20 ps and the remaining (20%) formed through the formation and thermal decomposition of ClOO.

Formation and Relaxation of ClOO. The possibility of ClOO formation in aqueous solution has been discussed for the past decade, but it was not until recently that it was observed directly following the photolysis of aqueous OClO.[41] Time-resolved resonance Raman (TRRR) spectroscopy of OClO following 390 nm excitation showed the appearance of ClOO 13 ± 2 ps after the photolysis pulse. The integrated scattering intensity of ClOO was best modeled by a sum of two exponentials resulting in an increase and decay time constant of 28 ± 5 ps and 0.40 ± 0.05 ns, respectively. The ClOO decay time constant of ∼0.4 ns was interpreted as thermal dissociation resulting in the formation of Cl and O_2, whereas vibrational relaxation most likely contributed to the ∼30 ps appearance kinetics.

Valuable information about the possible formation mechanism of ClOO from photoexcited OClO in aqueous solution may be obtained from high-level ab inito calculations on the electronic potential energy surfaces of ClOO, OClO, and their asymptotic correlation to product states. Arguments based on correlation diagrams in solution-phase photochemistry might be misleading, since studies of CS_2, for instance, have shown that selection rules pertaining to gas-phase dynamics become less stringent in solution phase.[49] Thus, the discussion below is only intended as a guide. The photolysis of OClO in the near-UV region is initiated by exciting from the $^2B_1$ ground state to the $^2A_2$ state, which couples to the nearby $^2A_1$ and $^2B_2$ states through spin−orbit and vibronic interactions.[28] In the liquid phase these processes are thought to be faster than the reactive changes, so that the photochemistry of OClO originates from the $^2B_2$ state, where the three competitive reactions 1−3 take place.[30−33] Cl atoms can thus be produced from the electronically excited $^2B_2$ of OClO via two allowed reaction channels. The first mechanism occurs by direct asymmetric photoisomerization of OClO to ClOO. Under C_s symmetry, the lowest excited state of OClO ($^2B_2$) only correlates with an excited state of ClOO and not the $^2A''$ ground state.[7,26,28] Therefore, direct isomerization of photoexcited OClO results in the formation of excited-state ClOO which can decay to form Cl($^2P_2$) and $O_2(^1\Delta_g)$ or $O_2(^3\Sigma_g^-)$. However, excited-state internal conversion of ClOO to the ground-state A″ surface can precede dissociation in which case Cl($^2P_2$) and $O_2(^3\Sigma_g^-)$ are formed by ground-state decom-

(47) Otto, B.; Schroeder, J.; Troe, J. *J. Chem. Phys.* **1984**, *81*, 202−213.

(48) Kühne, T.; Vöhringer, P. *J. Chem. Phys.* **1996**, *105*, 10788−10802.

(49) Thomsen, C. L.; Madsen, D.; Thøgersen, J.; Byberg, J. R.; Keiding, S. R. *J. Chem. Phys.* **1999**, *111*, 703−710.

position of ClOO.[27] The second mechanism involves symmetric dissociation along a C_{2v} reaction coordinate producing also Cl($^2P_2$) and $O_2(^1\Delta_g)$ or $O_2(^3\Sigma_g^-)$.[28]

The femtosecond transient absorption data presented here demonstrate that atomic chlorine is produced on two separate time scales: the majority (80%) is observed within 20 ps, whereas the remaining (20%) is produced on a much longer time scale as a result of thermal decomposition of ClOO. The observation of the majority of the Cl atoms within 20 ps is in agreement with the previously proposed model for production of Cl atoms, which involved a short-lived unidentified precursor for the Cl formation.[38,39] The short-lived Cl atom precursor absorbs strongly between 220 and 300 nm, and an extinction coefficient of this species comparable to that of ClOO has previously been obtained using a simple kinetic model.[38,39] However, the absorption spectrum derived for this component differs significantly from the ground-state absorption spectrum of ClOO shown in Figure 1 and the precursor was therefore not assigned to ClOO. Instead, it was proposed that the precursor was an excited state of OClO approaching a configuration resembling that of ClOO before dissociating into Cl and O_2.[38] The observation of a precursor for the Cl production together with the correlation diagram discussed above makes it tempting to propose that the excited state of ClOO is the precursor for the direct chlorine production. However, ab initio calculations indicate that all the excited states of ClOO are dissociative[27] and will therefore probably dissociate into Cl and O_2 on a much shorter time scale than 6 ps. This directly addresses the next issue, the formation of ground-state ClOO. The direct formation of ClOO in the electronic ground state from the excited $^2B_2$ state of ClO_2 is intriguing, because the correlation diagram based on orbital symmetry suggests that ClOO should be formed in an excited state, and the excited states of ClOO are thought to be dissociative.[7,26,28] It is therefore doubtful if excited-state internal conversion of ClOO to the ground-state A″ surface can precede dissociation. Hence, recombination of Cl and O_2, which is known to yield ClOO in the gas phase, would seem a more likely source of ground-state ClOO.[22,25] The possibility that ClOO can be formed by geminate recombination of ClO + O is excluded, since the time delay for ClOO appearance was found to be 13 ± 2 ps in the TRRR experiment, substantially slower than the subpicosecond time scale for ground-state OClO formation.[41]

Both mechanisms for ClOO formation, excited-state internal conversion and geminate recombination of Cl and O_2, result in production of vibrationally excited ground-state ClOO in agreement with the present observation and the TRRR data. The proposed interpretation of the data is not conclusive and the initial mechanism of the photolytic formation of Cl atoms and ClOO from aqueous OClO remains unidentified with additional work required to address this issue.

Conclusions

The femtosecond data presented here represent the first direct measurement of the quantum yield of the ClOO formation in aqueous solution, and significantly clarify the role of this species in the mechanism for chlorine formation following the photolysis of OClO. The main result of the investigation presented here is that, in contrast to previously reported results, chlorine atoms are formed through two competing reaction channels. The quantum yield for ClOO and Cl formation was estimated using a transient absorption spectrum obtained at 50 ps to be 2 ± 1% and 8 ± 2%, respectively, whereas the quantum yield for ClO was estimated to be only 3 ± 2%. The lifetime of ClOO was found to be ~0.32 ns in very good agreement with the lifetime found for ClOO in aqueous solution using time-resolved resonance Raman spectroscopy. Furthermore, the solution-phase spectrum of ClOO was found to be very similar to that obtained in amorphous ice. The dissociation of ClOO was found to result in formation of Cl and O_2 in agreement with that the barrier for thermal dissociation along the Cl−O coordinate estimated to be only 0.26 eV. The spectrum obtained at the longest delay investigated (0.46 ns) could be reproduced assuming a total quantum yield for Cl formation of 10 ± 3% and quantum yield for ClO formation of 3 ± 2%. This result supports the assumed relationship between the decay of ClOO and the formation of Cl at long delays. The analysis also shows that most (87 ± 5%) of the photoexcited OClO molecules in aqueous solution reform via geminate recombination in agreement with previous studies. The analysis of the time evolution of the transient observed between 280 and 220 nm indicates that ClOO might be formed with excess vibrational energy. The observation of excess vibrational energy is in good agreement with the proposed mechanism for production of ClOO, with ground-state ClOO formed via internal conversion from the excited state or via geminate recombination of Cl and O_2.

Acknowledgment. The authors would like to thank Jan Thøgersen and Jørgen R. Byberg for many stimulating discussions during the course of this work. Furthermore, the authors are grateful to the Danish National Science Research Council for financial support. P.J.R. would like to acknowledge the National Science Foundation for their support of this work through the CAREER program (CHE-9701717). P.J.R. is a Cottrell Fellow of the Research Corporation and an Alfred P. Sloan Fellow.

JA002148O